Available online at www.sciencedirect.com
ScienceDirect
Trans. Nonferrous Met. Soc. China 34(2024) 246−254
Transactions of Nonferrous Metals Society of China
www.tnmsc.cn

Interfacial structures and their effect on thermal conductivity and mechanical properties of diamond/Cu−B composites

Zhong-nan XIE[1,2,3], Hong GUO[1,2,3], Wei XIAO[1,2,3], Xi-min ZHANG[1,2,3], Shu-hui HUANG[1,2,3], Ming-mei SUN[1,2,3], Hao-feng XIE[1,2,3]

1. State Key Laboratory of Nonferrous Metals and Processes, GRINM Group Co., Ltd., Beijing 100088, China;
2. GRIMAT Engineering Institute Co., Ltd., Beijing 101407, China;
3. General Research Institute for Nonferrous Metals, Beijing 100088, China

Received 21 June 2022; accepted 14 March 2023

Abstract: Different interfacial structures of diamond/Cu composites were synthesized by varying the boron (B) content. The microstructural, thermal, and mechanical properties of the composites were investigated. The results showed that diamond/Cu−B composites had a high thermal conductivity of 695 W/(m·K) and high bending strength of 535 MPa attributed to the formation of a micron-scale dentate B_4C interface structure. The dentate B_4C provided dual functions of metallurgical bonding and mechanical meshing for interface bonding. A semi-coherent interface was formed between the diamond and B_4C, where the diamond (111) and B_4C (104) planes were parallel. The micro/nano-scale dentate structure improved the phonon transmission efficiency and bonding strength at the interface.

Key words: metal matrix composites (MMCs); diamond/Cu composites; thermal conductivity; interfacial structures

1 Introduction

With the rapid development of high-power electronic equipment, there is a great demand for advanced thermal management materials for heat sinks and microelectronic applications [1,2]. Carbon materials (including diamond, graphene, and carbon nanotube) reinforced metal matrix composites exhibited excellent thermal conductivity in previous studies [3−5]. Among these candidates, diamond-reinforced copper matrix composites (diamond/Cu) are promising for the heat dissipation of high-power chips due to their excellent thermo-physical properties and tunable thermal expansion [6]. However, carbon and copper neither wet nor react, even at high temperatures, due to the differences in their physico-chemical properties. These properties usually result in a poor interface between diamond and copper, further affecting the heat conduction and load transmission at the interface [7,8].

Studies have employed several routes for interface improvement to reduce the impact of weak interfaces on the thermal conductivity and mechanical properties of diamond/Cu composites. Under severe high-temperature and high-pressure preparation conditions, diamond/Cu composites might achieve coherent interfaces. YOSHIDA and MORIGAMI [9], and EKIMOV et al [10] have systematically addressed the impacts of numerous factors. The results indicated that polycrystalline diamond would be formed under high-temperature and high-pressure conditions, which is beneficial to eliminating interfaces and related defects. In addition, the fabrication of diamond/Cu composites with void-free interfaces by electroplating was proposed [11]. Although the perfect interface is the

Corresponding author: Hong GUO, Tel: +86-13601216895, E-mail: gh_grinm@126.com
DOI: 10.1016/S1003-6326(23)66395-2

goal pursued in diamond/Cu composites, harsh fabrication technology limits its application in industrial production.

Interfacial modification is another effective method that improves interface wetting and bonding remarkably. The carriers of heat transfer (i.e., phonons and electrons) control the heat transfer mechanisms in diamond and copper. The interface layer also acts as a phonon bridge between diamond and copper. CAO et al [12] introduced graphene as an interface layer that reduced the acoustic mismatch between diamond and copper, thus significantly improving the interfacial thermal conductivity. In addition, a new two-dimensional material MXene ($Ti_3C_2T_x$) adequately improved the interfacial thermal conductivity [13]. Furthermore, carbides of some elements (such as B, Cr, Ti, W, and Zr) improved wettability, interface thermal conductivity, and interface bonding strength between diamond and copper [14−18]. These carbides can transform the interface bonding into chemical bonding, which could significantly increase the thermal conductivity and interface bonding strength. CIUPIŃSKI et al [19] have prepared diamond/Cu composites, including Cr_3C_2 carbide via pulse plasma sintering, achieving the maximum thermal conductivity of 687 W/(m·K). As for boron, it can be directly alloyed into the copper matrix or grown on the diamond surface as a coating, resulting in increased tensile strengths and thermal conductivities compared to the systems without boron addition [8,14]. The highest thermal conductivity of 538 W/(m·K) was achieved with an optimal boron content of 0.8 wt.% [20].

In addition to the thermal conductivity, the mechanical properties of diamond/Cu composites are equally important for their application. ABYZOV et al [21] developed a diamond/Cu composite with high filler content (60 vol.%) and coarse diamond particles (180 μm), which exhibited a high bending strength of 380 MPa. ZHANG et al [22] obtained diamond/Cu−Zr composites with a bending strength of 440 MPa by zirconium interface modification. In previous work, 0.7 wt.% Cr addition achieved the highest tensile and bending strengths of 252 MPa and 523 MPa, respectively [15].

Studies have been focused on the scale effect of the carbide interface layer while ignoring the influence of the interface layer structure. In this work, diamond/Cu−B composites were prepared by vacuum pressure infiltration, and an in-situ generated micro/nano-scale dentate interface structure was discovered. The effects of different dentate structures on the thermal conductivity and strength of diamond/Cu−B composites were studied. The formation process of the micro/nano-scale dentate was analyzed by microscopic means to reveal the mechanism by which the dentate improves the interface phonon transmission efficiency and the interface bonding strength. Hence, this work provides valuable guidance for the design of high-heat conduction interface structures in diamond/Cu composites.

2 Experimental

Pressure infiltration was performed to prepare diamond/Cu composites with different boron contents. Copper bulks (purity of 99.9 wt.%) and boron powder (size of 2−3 μm, and purity of 99.99 wt.%) were obtained from Cuibolin Non-Ferrous Technology Co., China, and used as the composite matrix. Single crystal diamonds with a grain size of 100 μm were obtained from Huanghe Whirlwind Co. (China) and added to the composites in 60 vol.%. First, diamond particles were made into preforms and placed in graphite molds. Using the vacuum pressure infiltration method, Cu−B alloy (0.3 wt.%, 0.5 wt.%, 0.7 wt.%, and 1.0 wt.% of B) was poured into the graphite mold at 1250 °C. Mechanical pressure of 50 MPa was applied to forcing copper to penetrate the preform gap. The samples were kept at 1000 °C and 50 MPa for 60 min, and then the diamond/Cu−B composites with a diameter of 100 mm were obtained. The nitric acid etching was subsequently applied to exfoliating the diamond particles in the composite. Diamond/Cu−B composites were heated to 200 °C in 68 wt.% nitric acid for 30 min, and the diamond particles were obtained after the dissolution of the matrix copper.

The microstructures of diamond/Cu−B interfaces were analyzed using scanning electron microscopy (SEM, JSM−7610F Plus, Hitachi, Japan) and transmission electron microscopy (TEM, JEOL−2100F, Japan). Selected area electron diffraction (SAED) was used to examine the atomic structure at the interface of the diamond/Cu−B composites. The X-ray diffraction (XRD) patterns of diamond/Cu−B composites were recorded using the X'Pert-Pro MPD diffractometer (Holland Panalytical) with Cu K_α. The interface microstructure samples of diamond/Cu−B composites were prepared by focused ion beam etching. The thermal conductivity of diamond/Cu−B composites was calculated by

$$K=\alpha\cdot\rho_c\cdot c_p \tag{1}$$

where α, ρ_c, and c_p represent the thermal diffusivity, density and specific heat capacity of the composite, respectively. The thermal diffusivities of the diamond/Cu−B composites were measured at room temperature by a thermal conductivity tester (LFA447, NETZSCH). The densities of the diamond/Cu−B composites were measured by the drainage method. The measurement was repeated three times for each sample and averaged. The specific heat capacities of the composites were measured at room temperature by a synchronous thermal analyzer (STA 449F3, Netzsch, Germany). The bending strengths of the diamond/Cu−B composites were measured by a universal material testing machine. The testing sample size was 4 mm × 3 mm × 35 mm.

3 Results and discussion

3.1 Microstructures and phase constitutions

The nucleation and growth of interface carbide are affected by various conditions including temperature and boron content. By controlling these parameters, in-situ controllable growth of carbides can be achieved, and thereby different interface structures are prepared. The surface morphologies of the diamond particles extracted from diamond/Cu−B composites was examined by SEM, as shown in Fig. 1. When a small amount of boron was added, one-third of the exposed defects existed on the diamond surface. Upon increasing the boron content, the size of sparse carbide protrusions reached 1 μm. However, spot defects remained on the surface that was not covered with carbide. When the boron content reached 0.7 wt.%, a compact and uniform carbide layer was formed on the diamond surface, along with carbide dentate structures of a uniform size distribution of about 1 μm. Further increased boron content provided sufficient elements for carbide growth. Carbides continued to grow perpendicular to the diamond surface, with dentate structures up to 1.5 μm. With this structure, the dense carbide layer on the surface massively reduced the interface thermal resistance. Simultaneously, diffusion bonding and physical-mechanical meshing combined the dentate carbide and the matrix.

To confirm the composition of dentate carbide at the interface of diamond/Cu−B composites, the phase compositions of the polished surfaces (Fig. 2(a)) and the elemental composition of the near-interface region were measured by XRD and EDS. As depicted in Fig. 2(b), significant boron accumulation was detected near the diamond interface region, which indicates that boron diffuses from the copper−boron solid solution to the diamond during the infiltration process. Further, phase analyses have shown that a newly formed phase of B_4C was detected except for the copper and diamond phases in Fig. 3. Hence, it is confirmed that B_4C is the product of the interface reaction during the infiltration process of the diamond/Cu−B composites. The presence of B_4C enhances the interfacial bonding between diamond and copper, as inferred from the fracture morphology.

The fracture structures of the diamond/Cu−B composites with different boron contents are shown in Fig. 4. Increasing the boron content enhanced the proportion of diamond transgranular fractures within the fracture structure. When the boron content was lower than 0.5 wt.%, the fracture was dominated by diamond extraction. Part of the carbide adhered to the extracted diamond surface, and the uniform layer was not formed in carbide. Hence, carbides were insufficient to provide strong interfacial bonding. When the boron content was increased to 0.7 wt.%, the proportion of diamond transgranular fracture within the fracture increased, and more carbides adhered to the extracted diamond surface. Further enhancement of the boron content to 1.0 wt.% promoted transgranular fracture in the diamond, indicating that the interfacial bonding force became stronger.

3.2 Interface characterization

The interface microstructures of the diamond/Cu−B composites were revealed by TEM. High-resolution atomic images were obtained to reveal

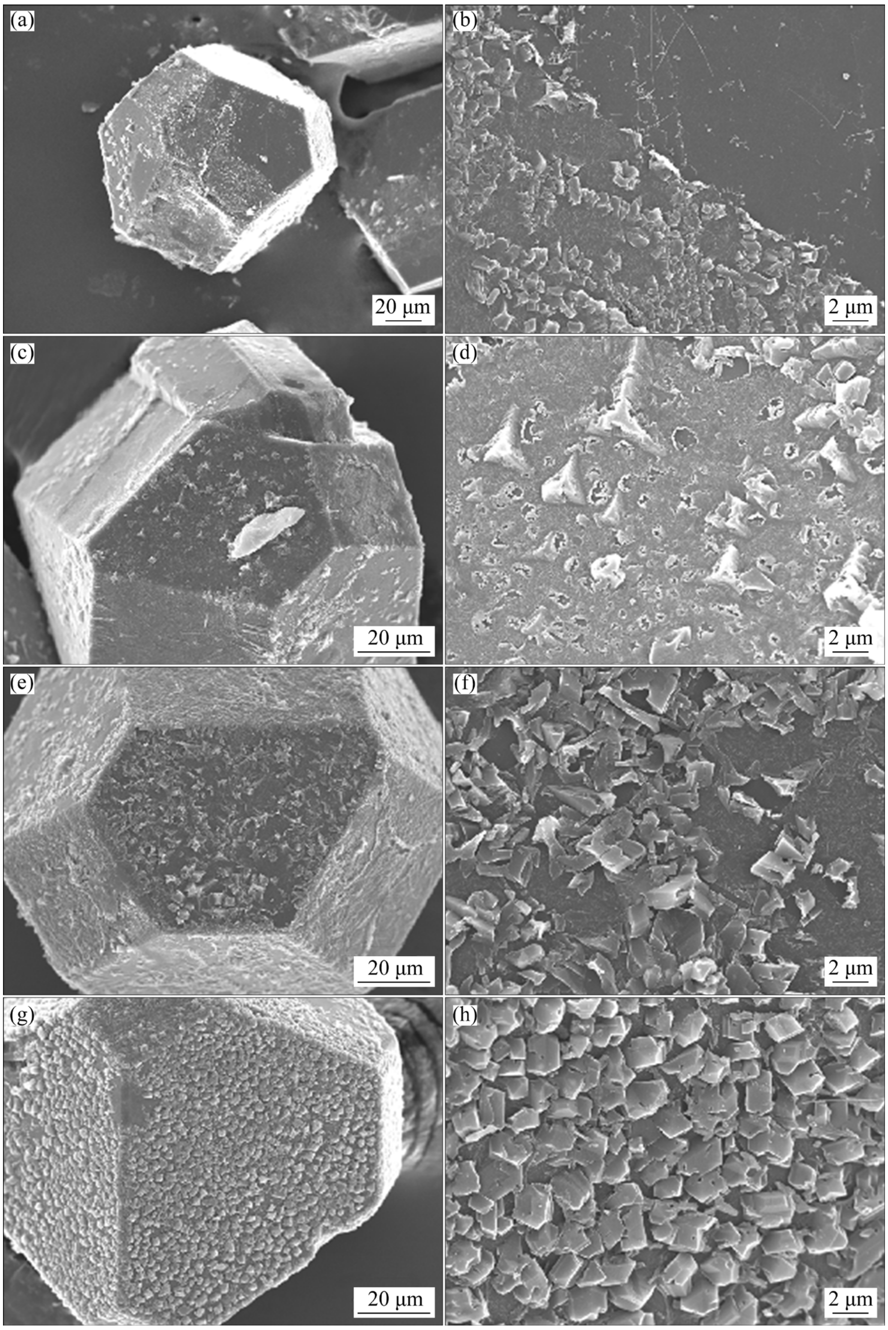

Fig. 1 SEM images revealing surface morphologies of diamond particles extracted from diamond/Cu−B composites at different boron (B) contents: (a, b) 0.3 wt.% B; (c, d) 0.5 wt.% B; (e, f) 0.7 wt.% B; (g, h) 1.0 wt.% B

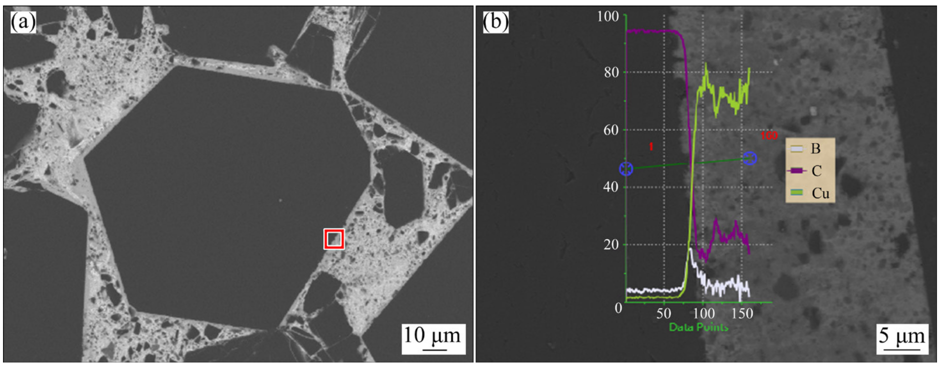

Fig. 2 SEM image for polished surface of diamond/Cu−B composites (a) and element analysis of interface area (b)

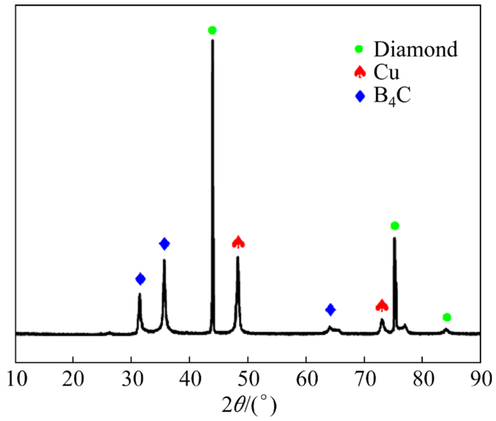

Fig. 3 XRD pattern of diamond/Cu−B composites

the interfacial bonding between diamond and B_4C. Figure 5(a) shows that a tooth structure appeared between the diamond and B_4C when the boron addition was 0.5 wt.%. With increasing the boron content, the tooth structure at the interface disappeared, as shown in Fig. 5(b). A straight and clear interface was formed between the diamond and B_4C. The diamond crystal planes parallel to the interface were designated as diamond (111) planes. The high-resolution atomic image in Fig. 5(c) shows that the dentate structure was composed of diamond atoms. The diamond crystal plane parallel to the interface was demarcated as the (111) plane with an interplanar distance of 0.206 nm. Interestingly, the orientations of the faces where the dentate structure binds to B_4C were all diamond (111) faces. Overall, these findings indicate the evolution of the interface between diamond and B_4C during the infiltration process in diamond/Cu−B composites.

Figure 5(e) graphically depicts the changes affecting the diamond surface and the interface microstructure evolution between diamond and B_4C during infiltration. Initially, the surface of the diamond particles was flat. Upon exposure to the molten Cu−B alloy, the carbon atoms on the diamond surface began to fall off along the diamond (111) surface. Since the surface energy of the diamond (111) plane is lower than the diamond (100) plane, it is easier for the (111) plane to participate in interface reactions [23,24]. The exfoliated carbon atoms reacted with the boron in the alloy to form B_4C while leaving pits on the diamond surface. With the progress of the interfacial reaction, a dentate structure was formed gradually by the pits on the surface. Then, the dentate reacted to form a flat interface until the boron in the alloy was consumed. Therefore, it is evident that the content of boron controls the interface structure between diamond and B_4C.

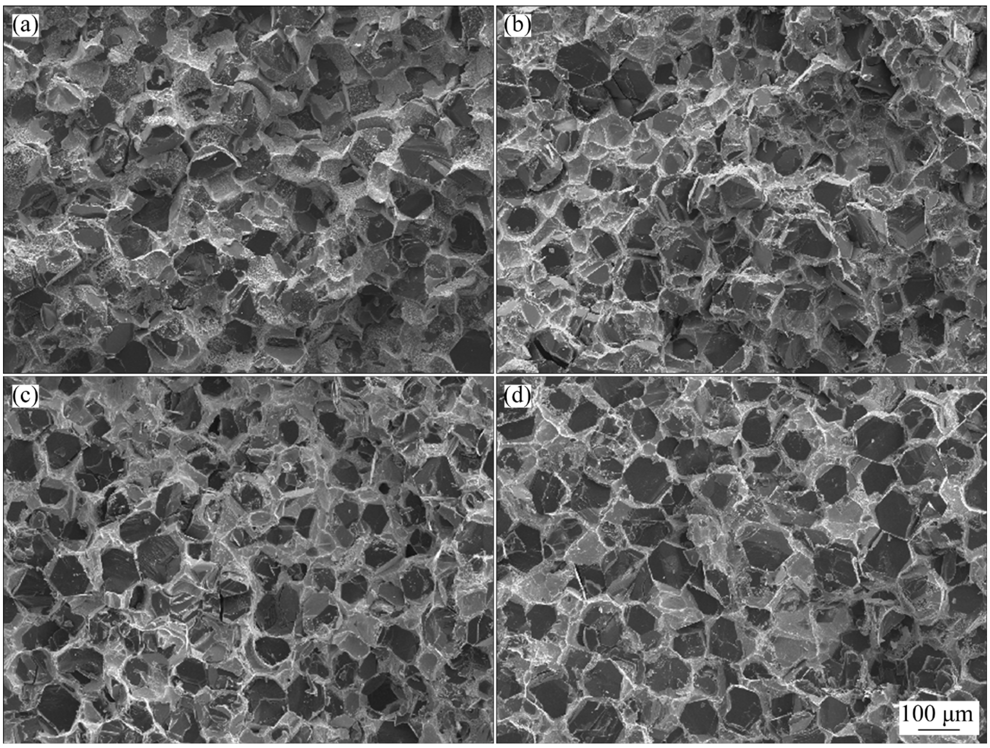

Fig. 4 SEM images for fracture morphologies of diamond/Cu−B composites at different boron contents: (a) 0.3 wt.% B; (b) 0.5 wt.% B; (c) 0.7 wt.% B; (d) 1.0 wt.% B

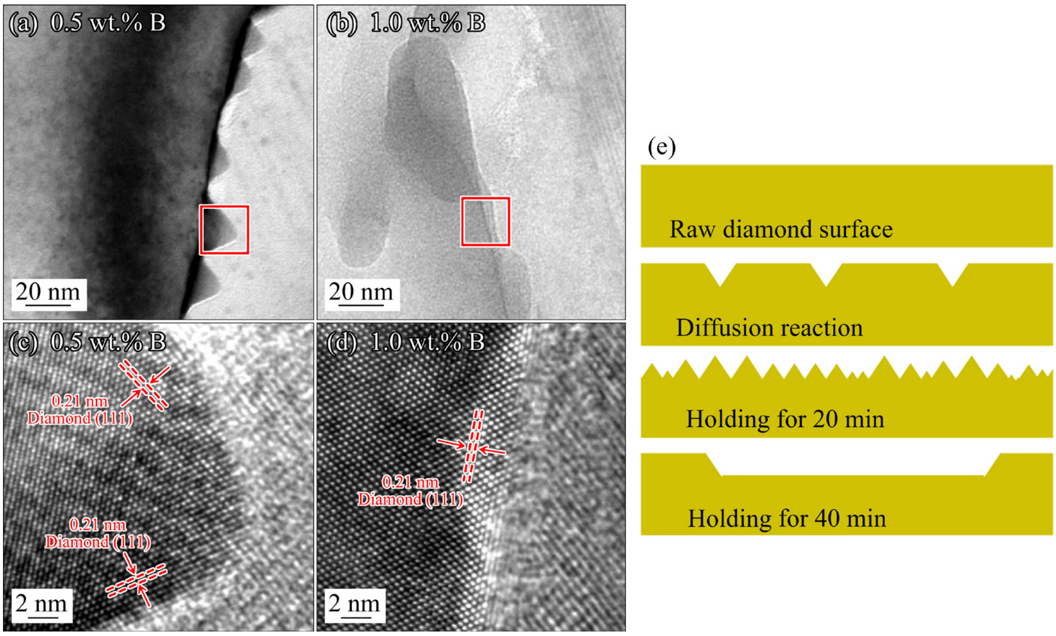

Fig. 5 TEM bright field images (a, b) and HRTEM images (c, d) of interface between diamond and B_4C in diamond/Cu−B composites; Schematic diagram of interface microstructure evolution between diamond and B_4C during infiltration (e)

To further reveal the micro-area heat transfer mechanism of the diamond/Cu−B composites interface, HRTEM and selected area electron diffraction (SAED) were used to analyze it. Figure 6(a) displays the bright-field image of the interface within diamond/Cu−B composites, where B_4C had an irregular shape with an average thickness of about 300 nm. The high-resolution atomic image of the b-region (Fig. 6(b)) shows that diamond (111) and B_4C (104) planes were parallel, i.e., diamond(111)//B_4C(104). Figure 6(c) shows that B_4C (104) plane was also parallel to the interface between B_4C and copper and that 10 nm copper nanocrystals were formed on the copper matrix side. SAED was performed on the selected areas in Fig. 6(a) and the corresponding SAED patterns are shown in Figs. 6(d−f). The results confirm that the d-region is diamond and the e-region is B_4C. The substrate side corresponding to the poly-crystalline ring is copper nanocrystals.

According to the interface atomic structure in Fig. 6(b), a schematic diagram of the interface bonding between diamond and B_4C was established, as displayed in Fig. 6(g). Based on the orientation relationship between diamond and B_4C, the lattice mismatch (δ) was calculated as 10.9%, where $\delta=(d_{\text{diamond}}-d_{B_4C})/(d_{\text{diamond}}+d_{B_4C})$, $d_{\text{diamond}(111)}$=0.206 nm, and $d_{B_4C(104)}$=0.256 nm [25]. The interface between B_4C and diamond is semi-coherent and the schematic diagram of the atomic matching model is shown in Fig. 6(g). The semi-coherent interface effectively reduced phonon scattering, thereby improving interface thermal conductivity. The schematic diagram of the interface phonon transport is shown in Fig. 6(h). However, the phonons reflected during phonon transmission in the tooth-shaped interface structure could re-enter the interface. Overall, this interface structure improved the phonon transmission efficiency, and thus it could also effectively improve the interface thermal conductivity [26].

3.3 Properties

The effect of boron content on the thermal conductivity of diamond/Cu−B composites is exhibited in Fig. 7. With increasing the boron content, the thermal conductivity firstly increased and then decreased, displaying a maximum value of 695 W/(m·K) at 0.7 wt.% boron content. The functional relationship between thermal conductivity and boron content can be interpreted by the interface structure. The thermal conductivity reached its highest value when the B_4C layer coated the diamond surface completely without defects.

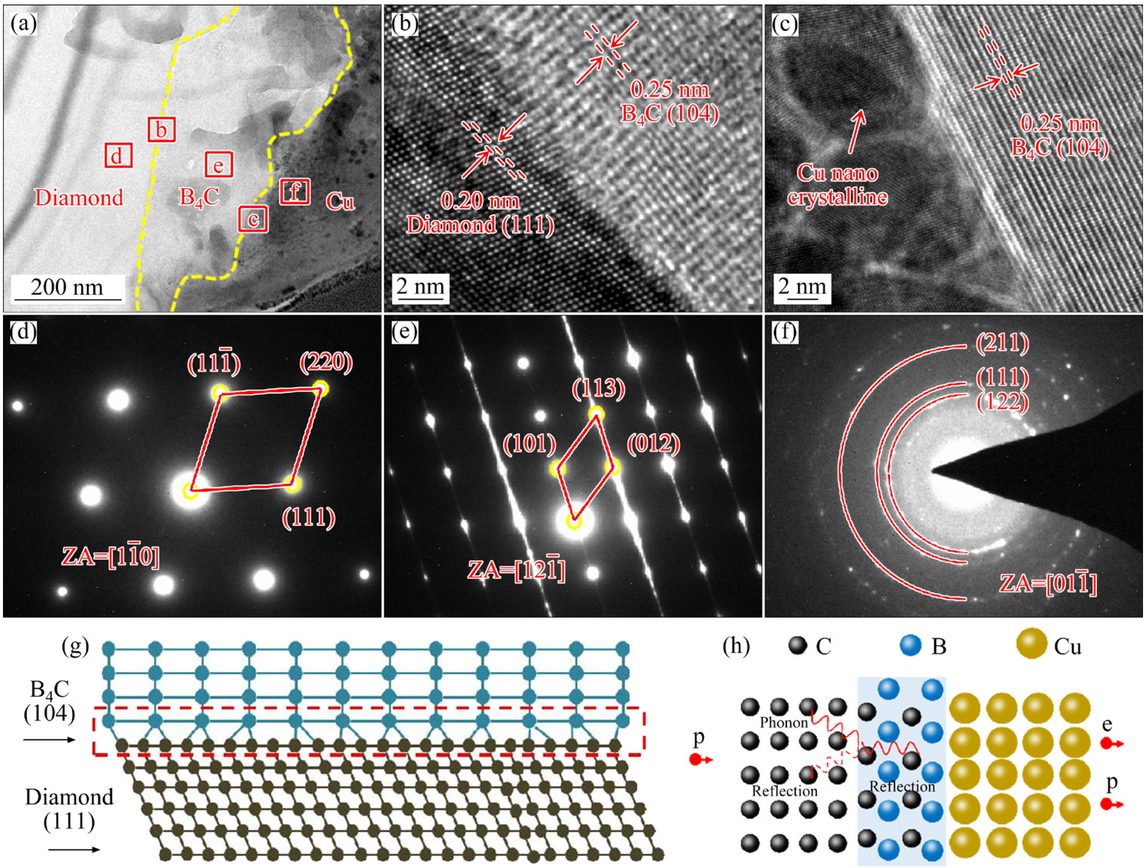

Fig. 6 TEM image of copper and diamond interface layer for diamond/Cu−B composites (a); High-resolution atomic image of interface between diamond and B_4C (b); High-resolution atomic image of interface between copper and B_4C (c); Selected area electron diffraction calibration of d-region (d), e-region (e), and f-region (f) in (a); Schematic diagram of interfacial bonding state between diamond (111) and B_4C (104) (g); Schematic diagram of interface phonon transport (h)

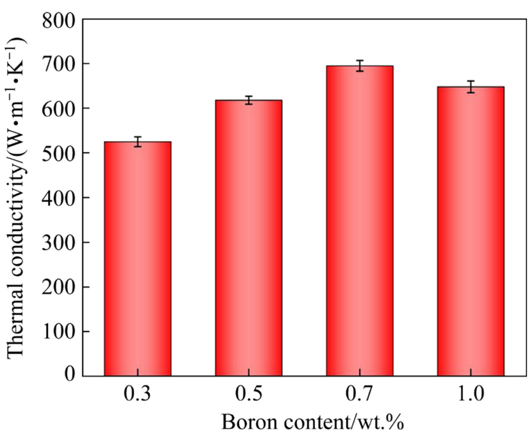

Fig. 7 Thermal conductivity of diamond/Cu−B composites with different boron contents

Beyond the critical value, increasing the B_4C layer grain augmented the interfacial thermal resistance. Therefore, further boron addition would decrease the thermal conductivity of diamond/Cu−B composites.

Figure 8 depicts the bending strength of diamond/Cu−B composites as a function of boron content. The bending strength of diamond/Cu−B composites increased linearly with the addition of boron content. Increasing the boron content from 0.3 to 1.0 wt.% enhanced the bending strength of the composites from 368 to 535 MPa. The bending strength of 535 MPa is higher than the previously reported value [22]. The improvement in bending strength is closely related to the strength of interface carbide and the near-interface area connecting diamond and copper. The size of B_4C continued to increase with the addition of boron content. The dentate B_4C extended to the matrix, forming mechanical engagement with the matrix, which significantly improved the bonding strength between the matrix and B_4C. Copper nano-crystalline regions were detected on the matrix side near the interface region. The nanocrystals enhanced the strength of the interface region, resulting in increased crack propagation resistance. Due to the stress concentration in the process of crack propagation, diamond transgranular fracture occurred. Therefore, the mechanical properties of diamond/Cu−B composites were significantly improved by controlling the process parameters to regulate the interface structure.

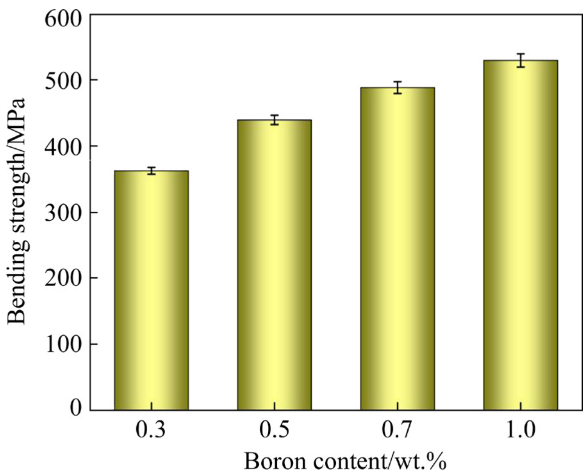

Fig. 8 Bending strength of diamond/Cu−B composites with different boron contents

4 Conclusions

(1) With increasing the boron content in the alloy from 0.3 wt.% to 1.0 wt.%, the carbide structure evolved from a discontinuous point-like structure to a dentate structure with 1.5 μm in height. The proportion of diamond transgranular fractures in the fracture structure of diamond/Cu−B composites continued to rise, which showed that the interface bonding strength increased with the change in the B_4C structure.

(2) By changing the boron content to tailor the B_4C structure, a maximal thermal conductivity of 695 W/(m·K) was obtained at 0.7 wt.% boron addition. However, a maximal bending strength of 535 MPa was attained at 1.0 wt.% boron addition.

(3) The micron-scale dentate B_4C structure provided the dual functions of metallurgical bonding and mechanical meshing for interface bonding. The interface formed between diamond and B_4C was semi-coherent and revealed the orientation relationship of diamond(111)//B_4C(104). The micro/nano-scale dentate structure improved the interface phonon transmission efficiency and interface bonding strength, thereby improving interface heat conduction and load transmission.

CRediT authorship contribution statement

Zhong-nan XIE: Conceptualization, Methodology, Writing − Original draft; **Hong GUO:** Conceptualization Funding acquisition; **Wei XIAO:** Writing − Review & editing; **Xi-min ZHANG:** Investigation; **Shu-hui HUANG:** Methodology; **Ming-mei SUN:** Validation; **Hao-feng XIE:** Funding acquisition

Declaration of competing interest

The authors declare that they have no known competing financial interests or personal relationships that could have appeared to influence that work reported in this paper.

Acknowledgments

This work was financially supported by the National Key Research and Development Program of China (No. 2017YFB0406202).

References

[1] IRADUKUNDA A C, HUITINK D R, LUO F. A review of advanced thermal management solutions and the implications for integration in high-voltage packages [J]. IEEE Journal of Emerging and Selected Topics in Power Electronics, 2020, 8(1): 256−271.

[2] TAO Jing-mei, ZHU Xin-kun, TIAN Wei-wei, YANG Peng, YANG Hao. Properties and microstructure of Cu/diamond composites prepared by spark plasma sintering method [J]. Transactions of Nonferrous Metals Society of China, 2014, 24(10): 3210−3214.

[3] ABYZOV A M, KIDALOV S V, SHAKHOV F M. High thermal conductivity composite of diamond particles with tungsten coating in a copper matrix for heat sink application [J]. Applied Thermal Engineering, 2012, 48: 72−80.

[4] CHU Ke, WANG Xiao-hu, LI Yu-biao, HUANG Da-jian, GENG Zhong-rong, ZHAO Xi-long, LIU Hong, ZHANG Hu. Thermal properties of graphene/metal composites with aligned graphene [J]. Materials & Design, 2018, 140: 85−94.

[5] KIM K T, ECKERT J, LIU Gang, PARK J M, LIM B K, HONG S H. Influence of embedded-carbon nanotubes on the thermal properties of copper matrix nanocomposites processed by molecular-level mixing [J]. Scripta Materialia, 2011, 64: 181−184.

[6] XIE Zhong-nan, GUO Hong, ZHANG Xi-min, HUANG Shu-hui. Enhancing thermal conductivity of Diamond/Cu composites by regulating distribution of bimodal diamond particles [J]. Diamond and Related Materials, 2019, 100: 107564.

[7] CHANG Guo, SUN Fang-yuan, DUAN Jia-liang, CHE Zi-fan, WANG Xi-tao, WANG Jin-guo, KIM M J, ZHANG Hai-long. Effect of Ti interlayer on interfacial thermal conductance between Cu and diamond [J]. Acta Materialia, 2018, 160: 235−246.

[8] SUN You-hong, HE Lin-kai, ZHANG Chi, MENG Qing-nan, LIU Bao-chang, GAO Ke, WEN Mao, ZHENG Wei-tao. Enhanced tensile strength and thermal conductivity in copper diamond composites with B_4C coating [J]. Scientific Reports,

2017, 7: 10727.

[9] YOSHIDA K, MORIGAMI H. Thermal properties of diamond/copper composite material [J]. Microelectronics Reliability, 2004, 44(2): 303−308.

[10] EKIMOV E A, SUETIN N V, POPOVICH A F, RALCHENKO V G. Thermal conductivity of diamond composites sintered under high pressures [J]. Diamond and Related Materials, 2008, 17(4/5): 838−843.

[11] WU Yong-peng, SUN Yun-na, LUO Jiang-bo, CHENG Ping, WANG Yan, WANG Hong, DING Gui-fu. Microstructure of Cu-diamond composites with near-perfect interfaces prepared via electroplating and its thermal properties [J]. Materials Characterization, 2019, 150: 199−206.

[12] CAO Huai-jie, TAN Zhan-qiu, LU Ming-Hui, JI Gang, YAN Xue-Jun, DI Chen, YUAN Meng-ying, GUO Qiang, SU Yi-shi, ADDAD A, LI Zhi-qiang, XIONG Ding-bang. Graphene interlayer for enhanced interface thermal conductance in metal matrix composites: An approach beyond surface metallization and matrix alloying [J]. Carbon, 2019, 150: 60−68.

[13] CAO Huai-jie, XIONG Ding-bang. Preparation of diamond/copper composites modified by $Ti_3C_2T_x$ as interlayer with enhanced thermal conductivity [J]. Diamond and Related Materials, 2021, 118: 108504.

[14] BAI Guang-zhu, ZHANG Yong-jian, LIU Xiao-yan, DAI Jing-jie, WANG Xi-tao, ZHANG Hai-long. High-temperature thermal conductivity and thermal cycling behavior of Cu−B/diamond composites [J]. IEEE Transactions on Components, Packaging, and Manufacturing Technology, 2020, 10(4): 626−636.

[15] XIE Zhong-nan, GUO Hong, ZHANG Xi-min, HUANG Shu-hui, XIE Hao-feng, MI Xu-jun. Tailoring the thermal and mechanical properties of diamond/Cu composites by interface regulation of Cr alloying [J]. Diamond and Related Materials, 2021, 114: 108309.

[16] ZHANG Yong-jian, BAI Guang-zhu, LIU Xiao-yan, DAI Jing-jie, WANG Xi-tao, ZHANG Hai-long. Reinforcement size effect on thermal conductivity in Cu−B/diamond composite [J]. Journal of Materials Science & Technology, 2021, 91: 1−4.

[17] LEI Lei, SU Yu, BOLZONI L, YANG Fei. Evaluation on the interface characteristics, thermal conductivity, and annealing effect of a hot-forged Cu−Ti/diamond composite [J]. Journal of Materials Science & Technology, 2020, 49: 7−14.

[18] WEBER L, TAVANGAR R. On the influence of active element content on the thermal conductivity and thermal expansion of Cu−X (X=Cr, B) diamond composites [J]. Scripta Materialia, 2007, 57(11): 988−991.

[19] CIUPIŃSKI Ł, KRUSZEWSKI M J, GRZONKA J, CHMIELEWSKI M, ZIELINSK R, MOSZCZYNSKA D, MICHALSKI A. Design of interfacial Cr_3C_2 carbide layer via optimization of sintering parameters used to fabricate copper/diamond composites for thermal management applications [J]. Materials & Design, 2017, 120: 170−185.

[20] CHU Ke, JIA Cheng-chang, GUO Hong, LI Wen-sheng. Microstructure and thermal conductivity of Cu−B/diamond composites [J]. Journal of Composite Materials, 2013, 47(23): 2945−2953.

[21] ABYZOV A M, SHAKHOV F M, AVERKIN A I, NIKOLAEV V I. Mechanical properties of a diamond-copper composite with high thermal conductivity [J]. Materials & Design, 2015, 87: 527−539.

[22] ZHANG Hai-long, QI Ying-xu, LI Jian-wei, WANG Jian-guo, WANG Xi-tao. Effect of Zr content on mechanical properties of diamond/Cu−Zr composites produced by gas pressure infiltration [J]. Journal of Materials Engineering and Performance, 2018, 27: 714−720.

[23] PIERRE M D L, BRUNO M, MANFREDOTTI C, NESTOLA F, PRENCIPE M, MANFREDOTTI C. The (100), (111) and (110) surfaces of diamond: An *ab initio* B3LYP study [J]. Molecular Physics, 2014, 112(7): 1030−1039.

[24] ZHANG Hong-di, ZHANG Jing-jing, LIU Yue, ZHANG Fan, FAN Tong-xiang, ZHANG Di. Unveiling the interfacial configuration in diamond/Cu composites by using statistical analysis of metallized diamond surface [J]. Scripta Materialia, 2018, 152: 84−88.

[25] JIANG Long-tao, WANG Ping-ping, XIU Zi-yang, CHEN Guo-qin, LIN Xiu, DAI Chen, WU Gao-hui. Interfacial characteristics of diamond/aluminum composites with high thermal conductivity fabricated by squeeze-casting method [J]. Materials Characterization, 2015, 106: 346−351.

[26] KOSEVICH Y A, FEHER A, SYRKIN E S. Resonance absorption, reflection, transmission of phonons and heat transfer through interface between two solids [J]. Low Temperature Physics, 2008, 34(7): 575−582.

金刚石/铜−硼复合材料界面结构及其对热导率和力学性能的影响

谢忠南[1,2,3]，郭 宏[1,2,3]，肖 伟[1,2,3]，张习敏[1,2,3]，黄树晖[1,2,3]，孙明美[1,2,3]，解浩峰[1,2,3]

1. 有研科技集团有限公司 有色金属结构材料制备加工国家重点实验室，北京 100088；
2. 有研工程技术研究院有限公司，北京 101407；3. 北京有色金属研究总院，北京 100088

摘 要：通过控制硼含量制备不同界面结构的金刚石/铜复合材料，研究复合材料的界面显微组织及其对热性能和力学性能的影响。结果表明，界面处形成微米级 B_4C 齿状结构，该结构为界面结合提供冶金结合和机械啮合的双重作用。金刚石/铜−硼复合材料获得最高为 695 W/(m·K)的热导率和 535 MPa 的弯曲强度。金刚石与 B_4C 之间形成具有金刚石(111)//B_4C (104) 取向关系的半共格界面。微纳米级齿状结构可提高界面声子传输效率和界面结合强度。

关键词：金属基复合材料；金刚石/铜复合材料；热导率；界面结构

(Edited by Bing YANG)